

# On Estimating Mote Operation Times During Typical Cross-Layer Functions

Sankarkumar Thandapani and Aravind Kailas

Dept. of Electrical Engineering

The University of North Carolina at Charlotte (UNC Charlotte)

9201 University City Blvd,

Charlotte, NC 28223-0001

Email: sthandap@uncc.edu, aravindk@ieee.org

**Abstract**—When it comes to deploying large scale, low power wireless networks comprising battery-operated embedded systems or motes, frequent replacement of batteries is undesirable. This motivates estimating the energy consumption in wireless motes accurately prior to deployment, and would avoid “sudden” decreased network coverage owing to pre-mature mote deaths. Using our proposed model, the energy consumption in the PHY layer was found to be within 10–15 % of the actual value obtained using measurements, and corresponded to an accuracy of 2–10% in the mote life. Furthermore, the cross-layer energy profiling involving the MAC layer provided insights into the energy consumed during the key modes of a simple, practical MAC protocol. To summarize, the primary purpose of this paper is to profile the energy consumption in a mote using a novel “off-line” model to predict its operation life with high accuracy.

**Index Terms**—Modeling and simulation of systems, practical medium access control protocols (MACs), energy efficiency

## I. INTRODUCTION

Most of the wireless motes are battery backed and are deployed in remote areas. Hence, replacing their batteries could be extremely difficult [1]. Accurate energy profiling of the motes still remains a key challenge in modeling the sensor networks [2]. The lifetime of sensor nodes may often be significantly shorter than expected. Szewczyk *et al.* found that their habitat-monitoring wireless network shrunk drastically due to mote failures within four days of deployment [3]. It has been observed that there were as many as 50 % of the wireless motes unexpectedly owing to inaccuracies in the energy consumption model. Thus, energy evaluation before deployment is extremely important. Hence, an accurate energy consumption model would help in avoiding expensive unexpected mote failures. The outcome of our research work is a simple, novel, system-level, “off-line” tool that accurately models the energy consumption exclusively in the PHY layer, (i.e., the transceiver (or the radio) and the micro controller

( $\mu$ C)) and a cross-layer energy consumption profiling involving the MAC layer. In areas involving commercial and scientific applications, low-power networks that operate in the industrial/scientific/medical (ISM) bands of 2.4 GHz are being widely adopted. Considering this, the effectiveness of the proposed model has been validated using commercial ZigBee-ready motes [4].

A wireless sensor network is composed of many sensor motes. A wireless mote comprises of transceiver,  $\mu$ C and sensor. In our paper, the PHY and the medium access control (MAC) layer are the focus areas for the energy consumption model. The classification of a transceiver would include radio frequency (RF) front-end (FE) and baseband processing back-end (BE). The front-end (FE) would in turn comprise of low noise amplifiers (LNAs), power amplifiers (PAs), mixers, filters, voltage controlled oscillators (VCOs), frequency synthesizers, intermediate frequency amplifiers (IFAs), automatic gain control (AGC) units, analog-to-digital converters (ADCs), and digital-to-analog converters (DACs) [5], [6]. The back-end (BE) comprises of blocks that perform functions as modulation, demodulation, error detection and correction, and pulse shaping.

The motes available in the industry are LOTUS [7], TelosB [8], MICAz [9], IRIS [10], CRICKET [11], etc. While deploying the mote, it is important to choose the right mote. It is remarked that measurements are necessary to validate the simulations, and there is the possibility to perform these measurements. However, it is very complex to measure the power directly and easier to simulate the energy consumption in a mote. It is necessary to treat the chip as one entity. In a simulation, the energy consumption of each block can be obtained and this information is useful when energy hogs in a mote needs to be studied. The proposed algorithm for modeling the energy consumption is “generic” in the sense that some of the more traditional receiver (e.g., low-power IF) and transmitter (e.g., direct-up

conversion) architectures that are very specific in their implementations [12].

The organization of the paper is as follows. Sections II and III describe the related state-of-the-art in predicting the energy consumption in wireless motes, and the novel energy consumption model. In Section IV, the experimental setup, methodology, and the results are presented. Finally, Section V has the concluding remarks resulting from this work.

## II. RELATED WORK

Although recent research provides many system-level energy consumption models, the accuracy of the model and completeness still remains an open topic to research. For instance, Cui *et al.* developed an energy model for low-power wireless motes to analyze the best modulation technique and transmission strategy to minimize energy consumption [6]. However, the energy costs associated with the  $\mu\text{C}$  and the modulation techniques were not considered; using our model, we show that when the modulation technique is considered, the architecture of the transceiver changes and the energy consumption increases by approximately 100%. The power consumption of the  $\mu\text{C}$  is non negligible too [14]. Our energy model considers the  $\mu\text{C}$  energy model which results in the higher accuracy of predicting the lifetime of the mote. The simulator presented in [15] considers the energy profiling of the  $\mu\text{C}$  but there are problems such as over counting and under counting of instructions which has been eliminated in our model. An energy model based on the transceiver battery life has been presented in [1]; however, the model did not account for the power consumption in the modulator, filters, the ADC, and the DAC. Using our model, we show that the powers consumed by the ADC and DAC are 1.4 mW and 19.01 mW, respectively, and cannot be disregarded.

Another recent energy model took into consideration most of the RF FE blocks with the exception of the pulse shaping filter because it is usually very low relative to the other “energy-hogs” [5]. However, the model also did not consider other baseband functions such as modulation and coding. The energy consumption in the MAC layer has not been studied in any of the above mentioned works. Kohvakka *et al.* in [17] have shown that the energy consumption due to the MAC depends on the number of nodes and the beacon interval. Our analysis of the energy consumption due to the MAC layer shows the key energy consuming modes in a MAC protocol. To summarize, the energy profiling of the  $\mu\text{C}$  is important to accurately estimate the energy consumption in PHY layer. The model proposed in the paper takes into consideration the effects of the modulation technique

along with the baseband processing blocks, the  $\mu\text{C}$  and the MAC layer resulting in a more accurate and complete estimation of the lifetime of a mote.

## III. THE ENERGY CONSUMPTION MODEL

The proposed energy consumption model has been adapted to the on-chip radio architecture [18], [19] to accommodate the preferred modulation technique, offset-quadrature phase shift keying (O-QPSK) and is shown in Fig. 1. The energy equation of each block proposed by many researchers has been tweaked to accommodate them as a part of the whole chip. Parameters such as voltage, device dimensions, frequency, data rate are common to all components in the chip and do not vary. Hence, they can be considered as constant and the expression becomes a function of the variables.

### A. Physical Layer in a Wireless Mote

A PHY layer of the wireless mote mainly consists of the transceiver and the  $\mu\text{C}$ . The energy consumption in the PHY layer is given as:  $E_{\text{Mote}} = E_{\text{Transceiver}} + E_{\mu\text{C}}$ .

1) *The Transceiver:* We have used MICAz motes to validate our model because of their wide popularity and extensive use in the sensor network community. MICAz motes operate on 2.4 GHz, and support data rates of up to 250 kbps [18], [19]. The operating voltage range is 2.1 – 3.6 V [19], and traditionally has four distinct operation modes depending upon the power requirements. The system-level breakdown of the energy consumption in the RF transceiver is given by  $E_{\text{transceiver}} = \sum_i E_{\text{FE},i} + E_{\text{BE},i}$ , where  $i \in \{\text{Transmitter, Receiver}\}$ , and  $E_{\text{FE}}$  and  $E_{\text{BE}}$  denote the energy consumptions in the front- and back-ends, respectively.

The RF FE of a transmitter comprises of a DAC, low-pass filter (LPF), mixer, PA, and the BE is the digital spreader. Similarly, the RF FE of the receiver is made up of a ADC, IFA, band pass filter (BPF), mixer, and a digital despreader as the BE block. The frequency synthesizer (FS) is common to both the transmitter and receiver architectures. Therefore, a simple unified expression for the energy consumption in the transceiver

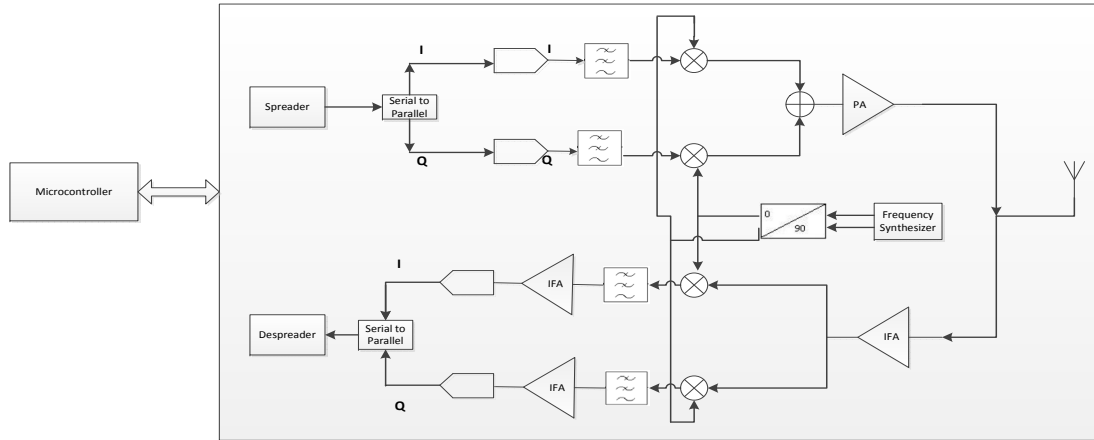


Fig. 1. Generic physical layer architecture of a wireless mote (a MICAz mote, in this paper).

is given by:

$$E_{\text{transceiver}} = t_{\text{tx}} \left[ \underbrace{P_{\text{Spreader}}}_{\text{BE, Transmitter}} + \underbrace{2P_{\text{DAC}} + 2P_{\text{LPF}} + 2P_{\text{Mixer}} + P_{\text{FS}} + P_{\text{PA}}}_{\text{FE, Transmitter}} \right] + t_{\text{rx}} \left[ \underbrace{P_{\text{Despreader}}}_{\text{BE, Receiver}} + \underbrace{2P_{\text{ACD}} + 2P_{\text{IFA}} + 2P_{\text{Mixer}} + P_{\text{FS}} + P_{\text{LNA}}}_{\text{FE, Receiver}} \right],$$

where  $t_{\text{tx}}$  and  $t_{\text{rx}}$  are the time durations during which the mote is operating in the transmitting or the receiving mode, respectively. Next, the simplified analytical models for the principle “power hogs” are listed:

- **Power amplifier:**  $P_{PA} = \alpha P_{\text{out}}$ , where  $\alpha$  is a constant that depends on efficiency of amplifier and peak to average ratio and  $P_{\text{out}}$  is the output power.
- **RF Filter:**  $P_{\text{Filter}} = \beta \text{SNR}^2 \text{BW}$ , where SNR is the signal to noise power ratio,  $\beta$  is a constant that depends on Boltzmann’s constant, the temperature, and BW is the bandwidth of operation.)
- **Low noise amplifier:**  $P_{LNA} = \gamma \frac{A}{\text{NF}}$ , where  $\gamma$  is the proportionality constant, A is the gain of the low noise amplifier, and NF is the noise figure.
- **Intermediate frequency amplifier:**  $P_{IFA} = \delta (\text{BW} + f_0) \sqrt{\alpha_{BA}}$  [5], where  $\delta$  is a coefficient

which depends on the device dimensions and process parameters, BW is the bandwidth of the baseband amplifier,  $f_0$  is the center frequency, and  $\alpha_{BA}$  is the baseband amplifier gain.

- **Spreader (and Despreader):**  $P_{\text{Spreader}} = P_{\text{XOR}} + NP_{\text{SR}}$ , where  $P_{\text{XOR}}$  is the power consumption of the XOR gate,  $P_{\text{SR}}$  is the power consumption of the shift register, and N is the number of shift registers.

2) *The  $\mu\text{C}$ :* The  $\mu\text{C}$  on a MICAz mote is ATmega128L, a low-power CMOS 8-bit  $\mu\text{C}$  based on the enhanced reduced instruction set computer (RISC) architecture. The energy consumption of a  $\mu\text{C}$  can be given as:  $E_{\mu\text{C}} = \frac{I * V * N}{F}$ , where  $I$  is the current supply,  $V$  is the voltage supply,  $N$  is the number of cycles,  $F$  is the frequency of operation.

The operating system on the MICAz is TinyOS. TinyOS is a free and open source component-based operating system and platform targeting wireless sensor networks. TinyOS applications are written in nesC, an extension to the C programming language designed to embody the structuring concepts and execution model of TinyOS. The nesC code has been converted into assembly language code, a low-level programming language for  $\mu\text{C}$ s using XATDB, the debugger of a sensor network simulator [21] in order to find the energy consumed by the  $\mu\text{C}$  while running the executable code. The assembly language code is used to compute the cycle count using XATDB and is substituted in the above equation. Data such as the supply voltage, supply current, and frequency of operation has been taken from the ATmega 128L data sheet [22]. The predicted energy consumption of the  $\mu\text{C}$  to run the executable code is 15 mJ.

B. MAC Layer in a Wireless Mote

The MAC protocol on a MICAz follows the IEEE 802.15.4 protocol [9], and supports two kinds of modes: beacon and non-beacon enabled. In a beacon enabled mode, the motes synchronize with each other and transmit only during their specified beacon. In a non-beacon mode carrier sense multiple access with collision avoidance (CSMA/CA) is used in order to avoid collision of the packets.

1) CSMA/CA: In CSMA/CA protocol, as soon as a node receives a packet that needs to be transmitted, it checks if the channel is available, and transmits it. If the channel is busy, the node waits for a randomly chosen period of time, and then checks again to see if the channel is available. If the channel is clear when the back-off counter reaches zero, the node transmits the packet. If the channel is not clear when the back-off counter reaches zero, the back-off factor is set again, and the process is repeated.

2) Beacon mode: It is an energy efficient mode and, hence choice for our model. The beacon enabled mode is used by motes to synchronize with each other. The communications are performed in a super frame structure illustrated in Fig. 2. There are three main parts in a super frame viz. the beacon, contention access period (CAP) and contention-free period (CFP). The nodes enter into power saving mode at the end of the super frame. The coordinators listen to the channel during the whole CAP to detect and receive any data from their child nodes. The child nodes may only transmit data and receive an optional acknowledgement (ACK) when needed.

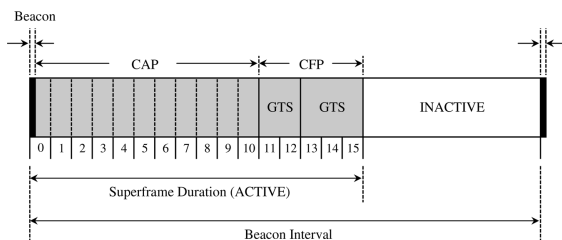


Fig. 2. Superframe structure (Beacon-enabled mode) implemented.

Contention access period (CAP) is the time interval during which the coordinators listens to the channel during the whole CAP to detect and receive any data from their child nodes. The child nodes may only transmit data and receive an optional acknowledgement (ACK) when needed. In star networks, a device may obtain better Quality- of-Service (QoS) by the use of guaranteed time slot (GTS), since contention and collisions are avoided. The superframe duration (SD) is the time interval be-

tween two super frames. Similarly the beacon interval (BI) is the time duration between two beacons.

3) Cross-Layer Energy Profiling: The energy consumption during a MAC mode is given by  $E_i = E_{i,Beacon} + E_{i,Direct} + E_{i,Indirect} + E_{i,Sleep}$ ,  $i \in \{mote, coordinator\}$ . In the **Beacon Mode** the transmitted beacon by the coordinator is received by the mote during this mode. In the **Direct Mode**, the mote exchanges data with the coordinator in its specified beacon slot. In the **Indirect Mode**, downlink data from a coordinator to its child node are sent indirectly requiring totally four transmissions. The availability of pending data is signaled in beacons. First, a child node requests the pending data by transmitting a data request message. The coordinator node responds to the request with ACK frame, and then transmits the requested data frame. Finally, the child node transmits ACK if the data frame was successfully received. A schematic of the start-topology is shown in Fig. 3.

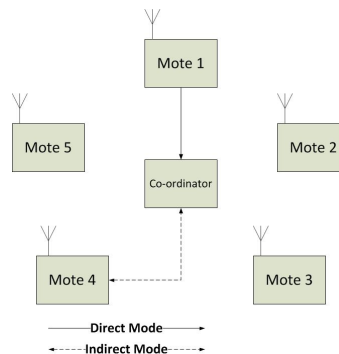


Fig. 3. Schematic of the star-network topology implemented using MICAz motes.

IV. RESULTS AND DISCUSSIONS

A. Experimental Setup

The energy consumption due to the PHY layer of the mote was verified experimentally. A source-destination link was implemented using MICAz motes as shown in Fig. 4. A payload of 20 bytes was transmitted by the source every 250 ms, and the base station (i.e., the destination) received payload at intervals of 250 ms. A sampling rate of 400 Hz was chosen to log the voltage and current consumption at the two motes to calculate the power consumption. The test consisted of 100 samples of current and voltage every second. The data was collected over a period of three days. The power consumed during a random hour was calculated and plotted with the simulation values. The samples obtained from the data logger were used to compute the power

consumption per sample, which were then averaged to obtain  $P_{\text{Transmitter}}$  and  $P_{\text{Receiver}}$ , the power consumed during the transmit and receive modes, respectively. The wireless motes were powered by two AA-sized batteries, each rated at 3000mAh [25], which when multiplied with the operating voltage yielded the initial residual energy, which in turn was used in the estimation of the mote operation life.

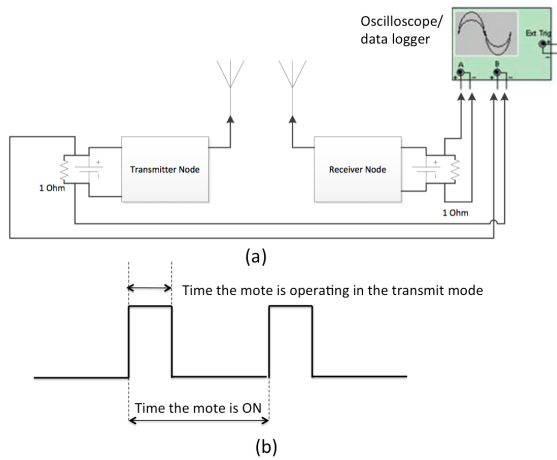


Fig. 4. (a) Illustration of the experimental setup and (b) timing diagram.

**B. PHY Layer Energy Consumption Analysis**

MATLAB [23] was used to implement the analytical model. The parameters for the transceiver model were selected from the CC2420 data sheet [19]. The energy consumption in the two modes of operation (transmit and receive) were estimated using the approach described in Section III. A, and the mote operation lives were compared to the experimentally measured values to validate the analytical model.

Figs. 5 and 6 illustrate the variation of residual energy (in mJ) with time of operation (in hours) at the transmitting and receiving motes, respectively. From Figs. 5 and 6, it can be observed that the energy consumptions of the transmitter and receiver obtained using our analytical model, are within 10.6% and 15% of the experimentally measured values. These differences can be accounted for by the light-emitting diodes (LEDs), battery leakage, on-board passive elements (i.e., resistors and capacitors) and voltage regulator that have not been considered in the analytical model.

The battery self discharge is negligible (typically 2–3% per month) in comparison to the discharge due to the load, and hence, neglected. Figure 7 illustrates the energy consumption (in mJ) for a certain payload, in the

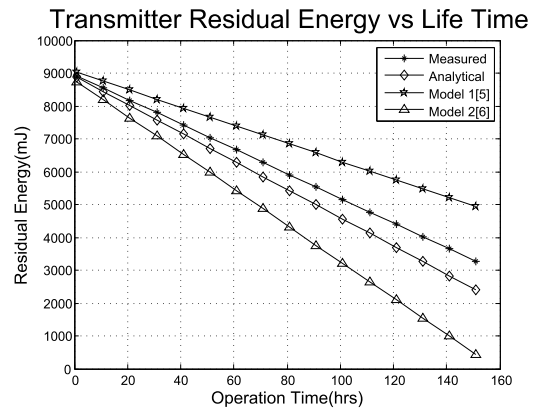


Fig. 5. Transmitter residual energy versus mote operation life (in hours).

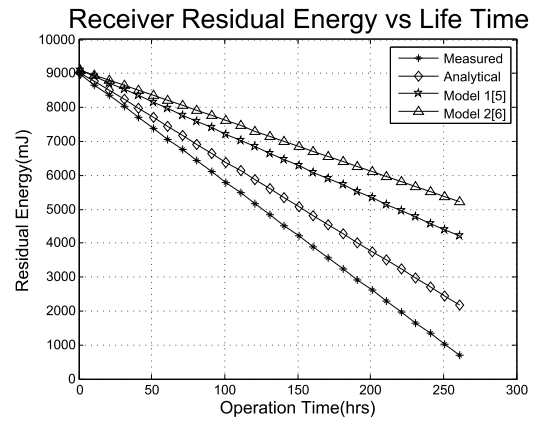


Fig. 6. Receiver residual energy versus mote operation life (in hours).

transmitting and receiving motes. The higher accuracy of the proposed model can be explained by the inclusion of the effects of digital modulation technique in the energy consumption computations along with the energy costs associated with the spreader (and de-spreader) and

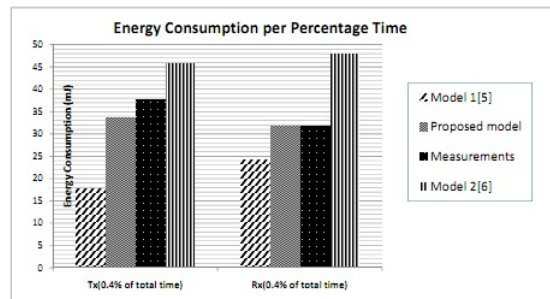


Fig. 7. Energy consumption of the transceiver for a 0.4% mode duration (i.e., transmit or receive).

$\mu$ C. The linear equation for the transmitter analytical model is given by  $\mathcal{R} = -33.678t + c$ , where  $\mathcal{R}$ ,  $t$ , and  $c$  denote the instantaneous residual energy on the battery, operation hours, and the total residual energy on the battery. The slope is the parameter that produces the change in the curve since the residual energy was assumed to be the same across the different models. Similarly, the equation of the receiver analytical model is given:  $\mathcal{R} = -26.332t + c$ .

C. Cross-Layer Energy Consumption Analysis

A star topology comprising five MICAz motes (referred to as the daughter motes) connected to a “coordinator” MICAz mote operating in the beacon-enabled mode. The energy consumption of each daughter mote is 1.25% of the coordinator mote, and is due to the higher duty cycle of the coordinator mote. Fig. 8 shows the time for the first mote and the coordinator to die. The burden of coordinating and being the “fusion” point for the cluster results in the coordinator node operating more, and hence dying earlier. While this should not be surprising, our analytical model helped predict this accurately and verifying this using our experiments. Next, the energy consumption of each mode in terms of the percentage of total energy consumption is given in Fig. 9. Again, not surprisingly, it can be seen that direct and indirect modes consumed the majority of the energy, again accurately predicted using our analytical model.

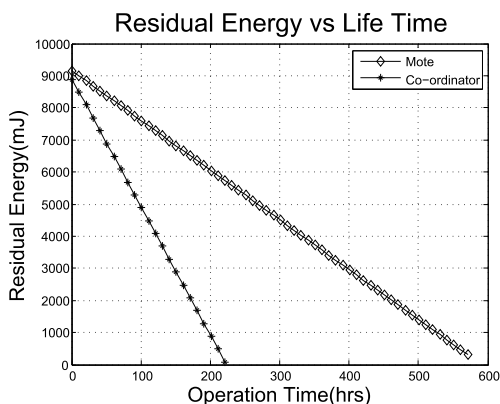


Fig. 8. Lifetime of the daughter and the coordinator motes

V. CONCLUSION AND FUTURE WORK

The wide-scale deployment of inexpensive wireless motes for networking hinges on accurately estimating the mote operation lives prior to deployment. Miscalculations in their estimations can prove costly, because of untimely, undesirable network partitioning. Using our

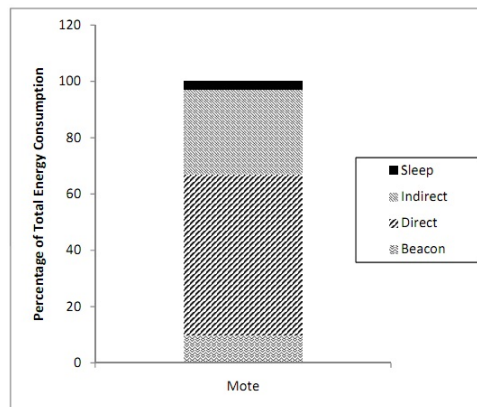


Fig. 9. Percentage of energy consumption per mode

unified, system-level energy consumption model, the predicted mote lives were found to be within 2–10% of the measured values. The high accuracy stems from the inclusion of the energy costs associated with the on-board functions such as control (i.e., the  $\mu$ C) and digital baseband processing (such as modulation, demodulation, spreading, and de-spreading).

By analyzing and expressing the results in terms of the three modes of operation of a mote (i.e., transmitting, receiving, and idle), our model gives better insights into the principle power hogs in the PHY layer of the mote during each mode. Furthermore, the cross-layer energy profiling involving the MAC layer provided insights into the energy consumed during the key modes of a simple, practical MAC protocol, and serves as motivation for future work in developing energy-efficient MAC protocols.

REFERENCES

- [1] A. Wang and C. Sodini, “A simple energy model for wireless microsensor transceivers,” *Proc. IEEE Global Telecommun. Conf. (GLOBECOM)*, vol. 5, Nov.–Dec. 2004, pp. 3205.
- [2] O. Landsiedel, K. Wehrle, and S. Gotz, “Accurate prediction of power consumption in sensor networks,” *The Second IEEE Workshop Embedded Networked Sensors (EmNetS-II)*, May 2005, pp. 37–44.
- [3] R. Szwedczyk, J. Polastre, A. Mainwaring, and D. Culler, “Lessons from a sensor network expedition,” 2004, pp. 307–322.
- [4] Available: <http://www.zigbee.org>. Retrieved: Aug. 2012.
- [5] Y. Li, B. Bakaloglu, and C. Chakrabarti, “A system level energy model and energy-quality evaluation for integrated transceiver front-ends,” *IEEE Trans. Very Large Scale Integr. (VLSI) Syst.*, vol. 15, no. 1, Jan. 2007, pp. 90–103.
- [6] S. Cui, A. Goldsmith, and A. Bahai, “Energy-efficiency of mimo and cooperative mimo techniques in sensor networks,” *IEEE J. Sel. Areas Commun.*, vol. 22, no. 6, pp. 1089–1098, Aug. 2004.
- [7] Available: <http://www.memsic.com/products/wireless-sensor-networks/wireless-modules.html>. Retrieved: Aug. 2012.

- [8] Available: <http://www.memsic.com/products/wireless-sensor-networks/wireless-modules.html>. Retrieved: Aug. 2012.
- [9] "MICAz Datasheet," 2004. [Online]. Available: <http://www-db.ics.uci.edu/pages/research/quasar/MPR-MIB%20Series%20User%20Manual%207430-0021-06A.pdf>. Retrieved: Aug. 2012.
- [10] Available: <http://www.memsic.com/products/wireless-sensor-networks/wireless-modules.html>. Retrieved: Aug. 2012.
- [11] Available: <http://www.memsic.com/products/wireless-sensor-networks/wireless-modules.html>. Retrieved: Aug. 2012.
- [12] P. -I. Mak, S. -P. U, and R. Martins, "Transceiver architecture selection: Review, state-of-the-art survey and case study," *IEEE Circuits Syst. Mag.*, vol. 7, no. 2, pp. 6–25, 2007.
- [13] X. Jiang, *et al.*, "Architecture for energy management in wireless sensor networks," *SIGBED Rev.*, vol. 4, pp. 31–36, July 2007. [Online]. Available: <http://doi.acm.org/10.1145/1317103.1317109>. Retrieved: Aug. 2012.
- [14] M. Kramer and A. Gerald, "Energy Measurements for MicaZ Node", Univ. of Kaiserslautern, Germany, 2006
- [15] V. Shnayder *et al.*, "Simulating the power consumption of large-scale sensor network applications," *Proc. 2nd Intl. Conf. on Embedded Networked Sensor Systems*, 2004, pp. 188–200.
- [16] G. Merrett, *et al.*, "An empirical energy model for supercapacitor powered wireless sensor nodes," *Proc. 17th Intl. Conf. Comput. Commun. Netw. (ICCCN)*, Aug. 2008, pp. 1–6.
- [17] M. Kohvakka, *et al.*, "Performance analysis of IEEE 802.15.4 and ZigBee for large-scale wireless sensor network applications," *Proc. 3rd ACM international workshop on Performance evaluation of wireless ad hoc, sensor and ubiquitous networks*, 2006, pp. 48–57.
- [18] N. -J. Oh and S. -G. Lee, "Building a 2.4-GHz radio transceiver using IEEE 802.15.4," *IEEE Circuits and Devices Mag.*, vol. 21, no. 6, pp. 43–51, Jan.–Feb. 2005.
- [19] "CC2420 Datasheet," 2004. [Online]. Available: <http://www.ti.com/lit/ds/symlink/cc2420.pdf>. Retrieved: Aug. 2012.
- [20] G. Bertoni, L. Breveglieri, and M. Venturi, "Power aware design of an elliptic curve coprocessor for 8 bit platforms," *Fourth Annual IEEE Int. Conf. Pervasive Comput. Commun. Workshops (PerComWorkshops)* Mar. 2006.
- [21] J. Polley, *et al.*, "ATEMU: a fine-grained sensor network simulator," *First Annual IEEE Com. Soc. Conf. on Sensor and Ad Hoc Communications*, pp. 145–152, Oct. 2004.
- [22] "ATmega 128L Data sheet," 2011. [Online]. Available: <http://www.atmel.com/dyn/resources/proddocuments/doc2467.pdf>
- [23] Available: <http://matlab.com>. Retrieved: Aug. 2012.
- [24] "TinyOS Application Code," 2010. [Online]. Available: <http://code.google.com/p/tinyos-main/source/browse/#svn%2Ftrunk%2Fapps%2FRadioSenseToLeds>. Retrieved: Aug. 2012.
- [25] "Energizer AA Battery Data sheet" 2010. [Online]. Available: <http://data.energizer.com/PDFs/191.pdf>. Retrieved: Aug. 2012.